19th International Conference on
Adaptive Structures and Technologies
October 6-9, 2008
Ascona, Switzerland

Multi-Layered Beams: Energy and Actuator Considerations

Gabriel Murray[1]*, Farhan Gandhi[2]
[1] The Pennsylvania State University, USA, 229 Hammond Building, University Park, PA 16802, Phone: 1-814-865-2469, Fax: 1-814-865-7092, gjm181@psu.edu
[2.] The Pennsylvania State University, USA

ABSTRACT

One purpose of a variable stiffness device is to reduced energy requirements. A variable stiffness beam design is investigated for this reduction in energy requirements. The strain energy is used as the energy required for actuation. The strain energy is investigated and provides insight into the physics of the variable stiffness beam. Coupling the strain energy with the heat required for polymer stiffness allows estimation of potential energy savings. Results show this is highly configuration dependent, with some of the best results using 10-20% of the stiff beam energy. These saving are only seen with stiff beam designs. Using an empirical relation, actuator mass shows significant reductions, with the stiff configuration requiring, on the order of 10-100 times, a more massive actuator.

Keywords: variable stiffness, energy reduction, mass reduction

1. INTRODUCTION

Previous work has focused on the testing and analysis of the variable stiffness concept investigated here [1,2]. The introductions of those papers discuss the various variable stiffness concepts, with a large majority having application in earthquake damage mitigation. For a complete compilation of variable stiffness devices, consult [1,2]. Here only energy and mass considerations will be discussed. While these designs are not actuated, they have energy associated with stiffness change. This energy is important, as in an earthquake external power cannot be relied on. In [3], the change in stiffness is achieved by decoupling supports from the main structure by using hydraulics. As a result, only 20W is needed to change the valve position. In [4], the change in stiffness is achieved by orienting springs with or at an angle to the load path. The 1:5 scale device uses 104W peak, to power a motor that results in the spring orientation changing.

Shape memory alloys and polymers undergo stiffness change as they are heated or cooled through their phase changes [5-9]. Similar to the concept of the variable stiffness beam, the energy required to enact stiffness change is heat, and this energy requirement can be quite large.

The reduction of actuator mass is independent on the method of variable stiffness and dependent solely on the stiffness change. This kind of benefit is only important when variable stiffness is applied to a system that is purposely deformed.

The current paper expands on the analytical study presented in [2]. As the analytical model has been previously presented, such details are only briefly reviewed. By considering the strain energy in the system and the heat required for polymer stiffness changes, a comparison between the energy required to deform the stiff beam and a softened beam are compared. Also, the reduction in

actuator mass that could be achieved by switching to a variable stiffness beam is also considered.

2. DESCRIPTION OF VARIABLE STIFFNESS BEAM AND ANALYSIS

Previous work [2] has discussed the concept of and methods used to analyze the variable stiffness beam, therefore only a brief review will be presented. The new analysis consists of determining the strain energy required to deform the beam as well as the energy required to heat the system, along with the reduction in the actuator mass of the softer system.

2-1. Concept of variable stiffness beam and analysis

The VSB is comprised of several layers, as in figure 1. The middle layer is the base beam, sandwiched by the polymer and cover layers, outwards respectively. The flexural stiffness of the beam is dependent on the shear stiffness of the polymer layer. With a stiff polymer layer, this layer undergoes little strain and the entire beam bends as an integral unit, resulting in a high flexural stiffness. With a soft polymer layer, this layer undergoes shear strain, decoupling the cover layers from the base beam, resulting in a lower flexural stiffness. Using a polymer with temperature dependent stiffness, the flexural stiffness of the beam can be changed in a quasi-static manner using heating or cooling.

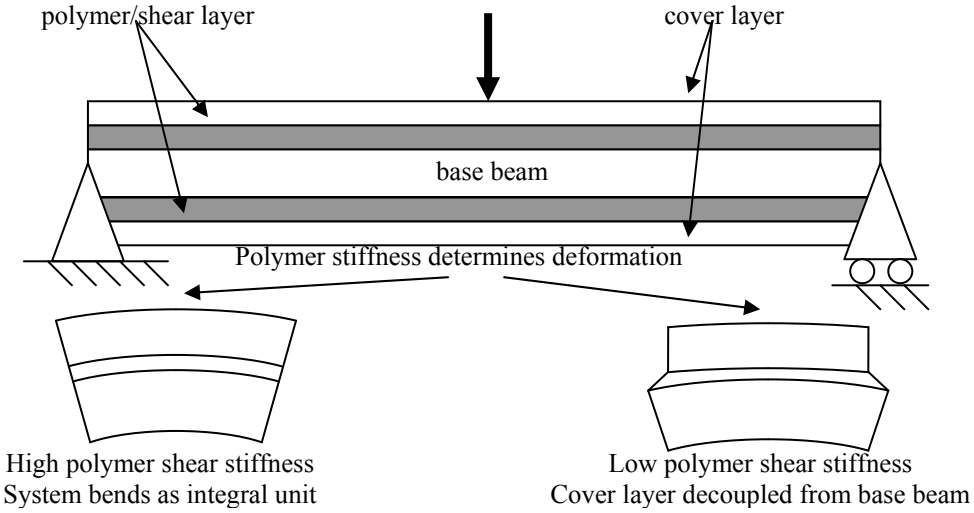

Figure 1. Schematic of variable stiffness beam

2-2. Analytical model description

The finite element method is used to analyze the system and the derivation and development of this model can be found in a previous work [2]. The finite element model modifies a standard beam element by adding a shear degree of freedom for the shear layer and by accounting for the additional kinematics introduced by the shearing polymer layer. The boundary conditions are simply-supported, with the base beam being pinned, and the load applied at the midpoint. To describe the beam configurations, a set of constant beam dimensions is defined, and nondimensional parameters are used to define the variable parameters, based on the base parameters. The dimensions are base beam's Young's Modulus, 70 GPa, length, 0.3 m, and width, 0.02 m. The definitions and ranges of the nondimensional parameters are given in table 1. The variations of β_G are representative of the changes in stiffness a polymer may undergo when heated. This is why the changes are three orders-of-magnitude, as this is a practical upper range for the stiffness change of polymers.

Table 1. Nondimensional parameters, their definitions and ranges

Parameter	Definition	Range
α_E	E_{cover}/E_{base}	0.1, 1, 10, 100
α_t	t_{cover}/t_{base}	0.01, 0.05, 0.1, 0.5, 1, 2
β_G	$G_{polymer}/E_{base}$	$10^{-4} \rightarrow 10^{-1}$
β_t	$T_{polymer}/t_{base}$	0.1, 0.5, 1
λ	L/t_{base}	20, 60, 100, 200

2-2-1. Energy analysis

Two different forms of energy are of concern: strain energy and heat. The former is calculated from the finite element results, whereas the latter is independent of the deformation. Strain energy is calculated using equation 1.

$$U = \frac{1}{2} q^T K q \tag{1}$$

This equation can be applied to the entire system, using the global displacement vector and stiffness matrix, or the strain energy in a layer of a particular element. By choosing the appropriate stiffness matrix and displacement vector, the desired strain energy is obtained. The heat required to raise the polymer's temperature is found using equation 2.

$$Q = mC_p \Delta T \tag{2}$$

This basic thermodynamic equation relates heat capacity and the material mass to give the heat required for a given temperature change. The mass of the polymer layers are determined using the volume and density of the polymer layer. There are several assumptions made in calculating the heat required. First, the polymer layer is assumed perfectly insulated and heated. As a result, heat is not lost with time and is independent of the beam's deformation. The density and heat capacity of extruded acrylic were chosen, 1190 Kg/m^3 and 1470 J/Kg-K, respectively. The change in temperature to achieve stiffness change is constrained to the transition region between the glassy and rubbery states of the polymer. The temperature change is 20 K, which can be found in shape memory polymers [9]. These values were chosen to give an idea of what is possible, but do not represent any particular material.

Having deformation independent heating makes larger deformations more advantageous when comparing strain energy with heat. Larger deformations do not require additional heat, but have larger strain energies, leading to more favorable energy ratios. The linear nature of the analysis provides the upper limit of deformation. ANSYS was used to give an estimate of the upper limit of deformation for the simply-supported boundary condition. A displacement 10% of the length at the midpoint results in errors less than 5% and is used as the maximum midpoint displacement. Another limit was required to ensure the shear angle was physically realizable, as in some configurations the displacement resulted in a shear angle greater than 90°. To prevent these physically inconsistent results a maximum shear angle of 45° was chosen. Therefore, results with deformation dependence (i.e., comparing the strain energy and heat) have to meet the two above limits.

2-2-2. Mass analysis

The stiffness of the beam always decreases as the polymer layer is softened. Correspondingly, the force required to deform the beam is reduced. The mass of the actuator can be related to the force using the empirical relation, equation 3 [10].

$$m = F^{1.49} \tag{3}$$

By introducing a force ratio of stiff over soft into F, a mass reduction ratio is obtained. The

strain energy ratios of the soft and stiff configurations are equivalent as shown in equation 4.

$$\frac{U_1}{U_2} = \frac{1/2\, q_1^T K q_1}{1/2\, q_2^T K q_2} = \frac{q_1^T F_1}{q_2^T F_2} = \frac{F_1 \delta}{F_2 \delta} = \frac{F_1}{F_2} \tag{4}$$

The equation of the strain energy can be simplified by substituting the relation between applied force and the stiffness matrix and displacement vector. Realizing the force vector has only one entry, at the midpoint, the only displacement that is multiplied by a nonzero term is the midpoint displacement. As both soft and stiff beams are deformed to the same displacement, the force ratio is equivalent to the strain energy ratio.

3. ENERGY AND STIFFNESS CONTRIBUTIONS

By plotting the strain energy in each element and differentiating the energy in each layer, the contribution of each layer to the total strain energy can be visualized. In addition, the two modes of deformation in the shear layer can be separated, namely shear energy and extensional energy. The layers with high strain energy indicate the areas with high strain and/or stiffness. The layers with the largest contribution to stiffness can be inferred from these results.

Left side of figure 2 shows the energy for each element and each layer for a representative soft polymer layer, pinned-pinned beam. The base beam and cover layer both have similar strain energy distributions and magnitude. The cover layer is further from the neutral axis and in an integral beam would have greater strain and strain energy. The similar strain energy levels are indicative of the cover layer bending as if attached side to side, instead of layered. The polymer layer is decoupling the cover layer from the beam, resulting in lower strain energy. The strain energy due to bending in the polymer layers is very small, as the polymer's low stiffness results in its paltry contribution. Nearly all of the energy in the cover layers is associated with shear, alluding to the large shear angles in the soft polymer layer as it shears to accommodate the cover layer. At the edges, the shear energy dominates the total energy (location of maximum shear), whereas in the middle the base beam dominates (location of minimum shear).

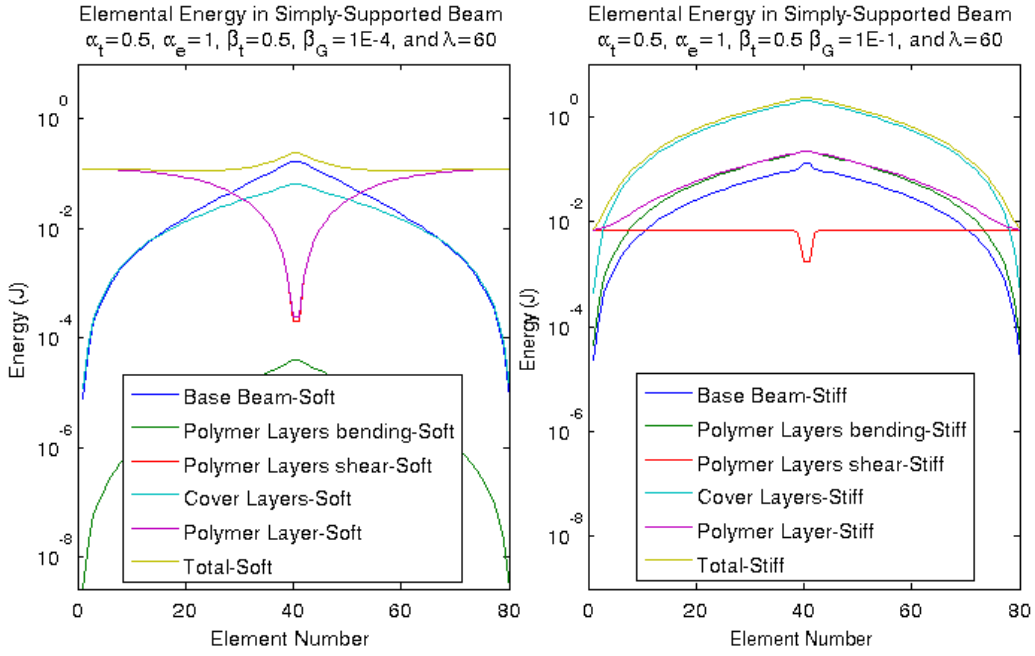

Figure 2. Elemental strain energy of soft (left) and stiff (right) polymer layers

Right side of figure 2 shows the strain energy for each element and layer of a representative stiff polymer layer simply-supported beam. The base beam only contributes a small amount of the

total strain energy, indicating the presence of a larger contribution to the strain energy (and stiffness). The cover layer strain energy is this predominate energy, indicating the cover layer is undergoing extension due to bending, due to strong coupling to the base beam. The cover layer is adding to the cross-sectional depth, greatly increasing the flexural stiffness of the beam. The extension due to bending in the polymer layer represents the majority of the strain energy in the shear layer. The domination of extension strain energy over shear strain energy in this layer is additional proof that the beam is bending as an integral unit. The polymer layer is no longer shearing to accommodate the cover layer. As a result of the small shear angle, the shear strain energy in the polymer layer is considerably smaller than the total polymer layer strain energy.

4. PARAMETRIC AND CASE STUDY RESULTS AND DISCCUSION

For the parametric studies, in order to assess the benefits of softening the beam, a total energy ratio of the strain energy and heat of the soft configuration over the strain energy of the stiff configuration is used. When this ratio is below 1, then it uses less energy to heat the beam beforehand. The actuator mass ratio is simply stiff over soft actuator masses. This was done so the values are always greater than 1.

4-1. Total Energy Ratio

The total energy ratio is dependent on the amount the beam deflects. The current model favors greater beam deflections giving more favorable total energy ratios. The table 1 contains the total energy ratio and is highlighted blue-green (darker) to show the beams that reach the maximum deflection limit of 10% of the length. The yellow (lighter) highlighted cells reach the shear angle limit before the deflection limit. The bold numbers indicate the smallest (or nearly so) total energy ratio for a particular slenderness ratio and cover layer thickness.

The results show that for many configurations, the addition of heat makes an enormous difference to the ratios' values. The majority of configurations show that heating the beam first uses more energy than bending the stiff beam, the high heat to strain energy is the reason. Only certain configurations, particularly those with stiff cover layers, have bending strain energy larger than the energy to heat.

For α_E=0.1 the lowest energy ratios are the configurations with the thickest cover layers, α_t=2. As the slenderness ratio decreases, the minimum energy ratio decreases, whereas the polymer layer thickness increases. For α_E=0.1, the only configuration with a total strain energy below 1 is the thickest possible configuration: lowest slenderness ratio, thickest cover and polymer layer. For this cover layer stiffness, the lowest energy ratio is 0.622.

For α_E=1, the same trends are seen. With the stiffer cover layer, a couple more configurations have an energy ratio below unity. However, these configurations all have low slenderness ratios and thick cover layers. These configurations emphasize the importance of having a stiff beam so the strain energy is larger than the heat required. For this cover layer stiffness, the lowest energy ratio is 0.177.

For α_E=10, there is a shift in the general trends. For the higher slenderness ratios, the thickest cover layer still gives the lowest energy ratio (0.121). Whereas, for the lowest slenderness ratio the lowest energy ratio has a thinner cover layer, half the thickness of the base beam.

For α_E=100, the above trend continues to develop. Only the highest slenderness ratio has the thickest cover layer giving the lowest energy ratio. As slenderness ratio decreases, the lowest energy ratio decreases and the cover layer thickness decreases. The lowest slenderness ratio configuration with the lowest energy ratio (0.103) has a cover layer thickness one-tenth that of the cover layer.

			Total Energy Ratio (α_E =0.1 & 1)			Actuator Mass Ratio (α_E =0.1 & 1)			Total Energy Ratio (α_E =10 & 100)			Actuator Mass Ratio (α_E =10 & 100)		
α_E	α_t	β_t	λ=200	λ=100	λ=60	λ=20	λ=100	λ=60	λ=20	λ=200	λ=100	λ=60	λ=20	λ=100	λ=60	λ=20
0.1 ‖ 10	0.01	0.1	165	41.87	15.60	2.47	1.326	1.326	1.326	96.67	24.80	9.426	3.095	1.194	1.256	1.384	2.153
		0.5	329.9	82.74	30.01	3.648	5.080	5.081	5.073	184.6	46.50	16.96	2.090	2.282	3.033	4.458	9.646
		1	234.9	58.87	21.31	2.528	22.71	22.69	22.38	144.3	36.30	13.19	1.602	4.275	7.382	13.67	36.20
	0.05	0.1	160.0	40.63	15.16	2.422	1.314	1.314	1.315	1.324	34.76	9.166	5.391	1.852	1.237	1.750	2.856	8.984
		0.5	319.2	80.08	29.07	3.549	4.637	4.653	4.685	4.924	64.59	16.34	5.973	0.768	2.485	6.437	14.85	42.25
		1	228.9	57.38	20.78	2.474	17.79	18.00	18.43	20.88	55.41	13.99	5.119	0.678	4.769	16.88	44.50	129.2
	0.1	0.1	153.4	38.98	14.57	2.351	1.298	1.299	1.303	1.335	18.38	5.399	4.730	1.150	1.430	2.649	5.496	22.04
		0.5	305.7	76.73	27.87	3.413	4.172	4.222	4.325	4.973	34.36	8.705	3.196	0.435	3.734	13.08	33.96	96.04
		1	221.4	55.52	20.13	2.400	13.83	14.38	15.46	20.79	30.57	7.745	2.862	0.419	7.989	35.37	99.00	258.3
	0.5	0.1	96.05	24.67	9.412	3.502	1.181	1.213	1.282	1.822	5.097	3.346	1.754	0.314	3.357	11.67	29.96	82.64
		0.5	204.2	51.44	18.78	2.322	2.346	2.738	3.525	7.367	5.364	1.389	0.538	**0.121**	17.75	74.74	156.9	164.7
		1	164.8	41.44	15.07	1.815	4.822	6.657	10.42	27.20	5.440	1.428	0.572	0.151	45.21	196.6	388.7	267.6
	1	0.1	47.29	12.47	4.971	4.489	1.110	1.202	1.404	3.105	4.782	2.377	1.054	0.242	5.364	16.77	30.41	37.41
		0.5	116.8	29.60	10.87	1.498	1.743	2.457	3.986	12.17	1.909	0.638	**0.289**	**0.138**	27.96	69.48	86.98	39.88
		1	110.0	27.75	10.11	1.241	3.025	5.474	10.92	36.86	2.141	0.598	**0.271**	0.147	68.66	157.02	171.1	47.53
0.1 ‖ 100	0.01	0.1	**14.19**	**4.151**	**4.930**	3.635	1.093	1.299	1.766	5.846	3.877	1.431	0.673	0.252	7.436	15.48	19.33	14.20
		0.5	42.74	11.01	**4.349**	**1.080**	1.566	2.810	5.535	18.21	**1.151**	**0.400**	**0.234**	0.267	25.436	33.89	30.18	8.89
		1	50.49	12.82	**4.709**	**0.622**	2.454	5.849	13.24	39.90	**0.739**	**0.259**	**0.171**	0.280	50.54	57.12	42.33	8.03
	0.05	0.1	155.0	39.38	14.71	2.367	1.301	1.303	1.306	1.334	20.80	5.534	4.737	1.151	1.428	2.612	5.309	19.66
		0.5	307.9	77.25	28.06	3.433	4.240	4.288	4.385	4.988	37.15	9.406	3.452	0.469	3.744	12.96	33.08	89.44
		1	222.2	55.72	20.20	2.408	14.19	14.73	15.79	20.94	32.17	8.149	3.011	0.440	8.038	35.36	98.03	249.2
	0.1	0.1	120.0	30.65	11.56	2.680	1.229	1.252	1.300	1.637	4.946	3.080	1.669	0.302	3.537	13.42	39.41	165.8
		0.5	234.6	59.02	21.50	2.642	2.738	3.121	3.849	6.832	7.934	2.038	0.777	0.149	20.29	103.3	280.7	482.6
		1	178.0	44.73	16.25	1.952	5.863	7.899	11.87	26.97	7.127	1.865	0.741	0.180	52.78	284.0	752.4	918.4
	0.5	0.1	90.76	23.33	8.892	3.351	1.184	1.250	1.389	2.259	3.935	1.917	0.939	0.176	6.940	32.53	99.69	352.3
		0.5	177.3	44.69	16.30	2.012	2.214	2.967	4.425	10.01	3.861	1.013	0.404	**0.103**	50.05	259.9	652.1	694.8
		1	141.0	35.46	12.89	1.566	4.121	7.169	13.43	36.83	3.556	0.968	0.416	0.141	133.9	690.2	1591	1095
	1	0.1	20.61	5.617	5.415	1.918	1.223	1.783	3.068	12.18	1.853	0.628	0.284	**0.125**	31.25	87.49	117.7	56.20
		0.5	46.02	11.68	4.285	0.563	2.366	6.298	15.14	48.34	0.594	0.191	**0.110**	0.134	182.3	294.6	229.1	33.03
		1	44.42	11.23	4.114	0.551	4.444	15.86	42.37	127.5	0.635	0.226	0.143	0.163	453.4	595.1	361.3	35.32
	0.5	0.1	6.999	5.477	4.895	1.149	1.403	2.592	5.354	21.11	1.161	0.391	0.228	0.239	30.14	42.68	38.61	11.07
		0.5	17.41	4.46	1.726	0.316	3.405	11.14	26.21	58.62	0.312	**0.148**	**0.138**	0.362	90.69	71.92	38.93	5.054
		1	19.11	4.863	1.809	**0.285**	6.961	27.64	66.05	119.3	0.292	**0.150**	0.148	0.393	181.2	106.8	45.32	4.685
	1	0.1	**4.793**	5.312	3.484	0.731	1.739	3.837	7.767	18.01	0.730	0.310	0.250	0.465	19.23	18.553	13.68	3.390
		0.5	**5.085**	**2.293**	**1.065**	**0.246**	5.172	15.04	25.49	29.10	**0.244**	0.203	0.278	0.696	31.14	17.38	8.207	1.761
		1	6.401	**1.674**	**0.663**	**0.177**	10.88	32.47	50.63	41.92	**0.175**	0.189	0.295	0.741	44.62	18.26	7.323	1.597

Table 2. Total strain energy and actuator mass ratio

4-2. Actuator Mass

Table 2 contains the results for the actuator mass ratios. The peak mass ratios for particular slenderness ratio and cover layer stiffness are highlighted in blue-green (darker). Whereas the values highlighted in yellow (lighter) represent the next closest values.

For α_E=0.1, the lowest slenderness ratio has the highest mass ratio (36.9) as well as the thickest cover layer. The maximum mass ratios of the other slenderness ratios have the thinnest cover layers. All share the commonality of having the thickness polymer layer.

For α_E=1, a trend can be seen that was not evident in the previous results. The greatest mass ratio (127.5) falls with the least slender beam, with a cover layer thickness half that of the base beam. As the slenderness ratio increases, so does the cover layer thickness for the largest mass ratio, whose values fall. With the exception of the most slender beam, however, it appears that if the maximum cover layer thickness was increased, the trend might continue. As before, all these values have the thickest polymer layer.

For α_E=10, maximum mass ratio (388.7) shifts to a slenderness ratio of 60. The lowest three slenderness ratio all share a common cover layer thickness half the thickness of the base beam. The most slender beam has a maximum mass ratio with a cover layer thickness that of the base beam.

For α_E=100, the same trend is seen, except the cover layer thickness ratio reduces to the next lower number, 0.1 and 0.5 respectively. The maximum mass ratio is 1591. The polymer layer thickness is the largest possible thickness. Considerable mass savings can be realized by softening the beam before deformation. The magnitude of the mass reduction is dependent on the configurations; all of the configurations provide a mass reduction, unlike with the total strain energy ratio. Such a relation is beneficial if energy usage is a major concern, concentrating on that ratio might result in a sub-optimum mass reduction, but a significant mass reduction is still achievable.

4-3. Case Studies

Two configurations will be looked at and discussed in detail. In particular, the values of the different ratios for a given configuration will be considered in a quantitative manner. Table 4 has the selected cases, with their configurations, and energy and mass ratios. The configurations were chosen based on physical realism (reasonable cover layer stiffness), as well as one having a low energy ratio and the other having a high mass ratio.

Table 3. Case study configurations and results

α_E	α_t	β_t	λ	$U_{soft}+Q/U_{stiff}$	m_{stiff}/m_{soft}
10	0.5	0.5	20	0.121	165
10	0.5	1	60	0.58	389

The first configuration was chosen for having the lowest total energy ratio for α_E=10. The second configuration was chosen for having the highest mass ratio (and by extension strain energy ratio) for α_E =10. A beam optimized for total energy ratio, is not optimized for mass ratio. There are two differences between the two beams. The second beam is more slender and has a thicker polymer layer, and these differences will be explored now. The increased slenderness ratio means the base beam of the second case is thinner, bringing the cover layers closer to the neutral axis. Increasing the polymer layer thickness moves the cover layer away from the neutral axis, but the net result moves the cover layer closer. The thicker polymer layer increases the difference in flexural stiffness between coupled and decoupled states, by allowing easier shearing and moving the cover layer further from the neutral axis, at the expense of increased heating requirements. Overall, the beam is softer in bending, but the difference between the states is greater. This increased heating requirement, coupled with decreased beam flexural stiffness, is the source of the increased total energy ratio when compared to the first beam. The first beam's thinner polymer layer requires less heat and the smaller slenderness ratio increases the base beam's flexural stiffness. Both traits add up to a smaller energy ratio.

5. CONCLUSIONS

Considering the energy, both strain and heating, of the VSB allows for further analysis of the beam's characteristics. Comparing the strain energy in different layers provides insight into which layers are providing the beam's stiffness. Looking at the polymer layer's dominate deformation mode reveals the effectiveness of the polymer in coupling or decoupling

Considering energy and heat allows for a comparison of potential energy savings. The calculation of heating energy is estimated using specific heat capacity. In certain conditions, especially with soft beams, the energy used to heat dominates the strain energy, even the stiff configuration's strain energy, resulting in an increase in energy consumption. In addition to having a stiffer beam, undergoing large deformations is beneficial to energy savings, as it increases the strain energy with out affecting the heating energy.

The VSB beam offers weight reduction in regards to the actuator. The reduction in stiffness allows for a lower maximum force actuator to be used. The weight of the actuator is related to the maximum force the actuator applies. As all beam configurations undergo a reduction in stiffness, they all experience a reduction in actuator weight.

Maximum energy savings and actuator mass reduction require different configurations. Therefore a balance between them may be required. Certain circumstances may result in one condition being more relevant than the other. The simple analysis done indicates that only certain configurations show an energy saving, certainly more extensive analysis will show a reduction in the configurations that offer savings.

REFERENCES

1. Gandhi, F., and Kang, S.-G., "Beams with Controllable Flexural Stiffness," *Smart Materials and Structures*, Vol. 16, No. 4, Aug. 2007, pp. 1179-1184.
2. Gandhi, F., Murray, G., and Kang, S.-G., "Flexural Stiffness Control of Multi-Layered Beams," 16th AIAA/ASME/AHS Adaptive Structures Conference, 7-10 April 2008, Schaumburg, Illinois, AIAA 2008-2205
3. Takahashi, M., Kobori, T., Nasu, T., Niwa, N., and Kurata, N., "Active Response Control of Buildings for Large Earthquakes – Seismic Response Control System with Variable Structural Characteristics," *Smart Materials and Structures*, 7, (1998) 522-529.
4. Nagarajaiah, S. and Sahasrabudhe, S., "Seismic response control of smart sliding isolated buildings using variable stiffness systems: An experimental and numerical study," *Earthquake Engineering and Structural Dynamics,*" **35**:177-197.
5. Otsuka, K., and Wayman, C. M., "Shape Memory Materials," Cambridge University Press, 1998, 1st Edition, pp 203-219.
6. Hodgson, D. E., "Using Shape Memory Alloys," Shape Memory Applications, Inc., Sunnyvale, CA, 1988.
7. Wei, Z., Sandstrom, R., and Miyazaki, S., "Review: Shape-memory materials and hybrid composites for smart systems," *Journal of Materials Science*, 33, 1998, pp. 3743-3762.
8. Lendlein, A., and Kelch, S., "Shape-Memory Polumers," *Angewandte Chemie International Edition*, **41**, 2002, pp. 2034-2057.
9. Atli, B., Gandhi, F., and Karst, S., "Thermomechanical Characterization of Shape Memory Polymers," *Proceedings of SPIE, Electroactive Polymer Actuators and Devices 2007*, 2007,
10. Marden, J., "Scaling of maximum net force output by motors used for locomotion," *The Journal of Experimental Biology*, 208, pp. 1653-1664